SAE International Journal of Commercial Vehicles, Vol.10, Iss.1, pp254-264
SAE TP 2017-01-0426
http://papers.sae.org/2017-01-0426/

2017-01-0426

Cyber-Physical System Based Optimization Framework for Intelligent Powertrain Control

Chen Lv, Hong Wang, Bolin Zhao, Dongpu Cao, Wang Huaji, Junzhi Zhang, Yuting Li and Ye Yuan.

Abstract

The interactions between automatic controls, physics, and driver is an important step towards highly automated driving. This study investigates the dynamical interactions between human-selected driving modes, vehicle controller and physical plant parameters, to determine how to optimally adapt powertrain control to different human-like driving requirements. A cyber-physical system (CPS) based framework is proposed for co-design optimization of the physical plant parameters and controller variables for an electric powertrain, in view of vehicle's dynamic performance, ride comfort, and energy efficiency under different driving modes. System structure, performance requirements and constraints, optimization goals and methodology are investigated. Intelligent powertrain control algorithms are synthesized for three driving modes, namely sport, eco, and normal modes, with appropriate protocol selections. The performance exploration methodology is presented. Simulation-based parameter optimizations are carried out according to the objective functions. Simulation results show that an electric powertrain with intelligent controller can perform its tasks well under sport, eco, and normal driving modes. The vehicle further improves overall performance in vehicle dynamics, ride comfort, and energy efficiency. The results validate the feasibility and effectiveness of the proposed CPS-based optimization framework, and demonstrate its advantages over a baseline benchmark.

Introduction

The ever-growing attention to the environment and energy conservation requires automobiles to be cleaner and more energy efficient. Technologies such as powertrain electrification and alternative fuels are being actively researched and developed. Among these solutions, various types of electrified vehicles with alternative power sources, including battery electric vehicles (BEVs), hybrid electric vehicles (HEVs), plug-in hybrid electric vehicles (PHEVs), and fuel cell electric vehicles (FCEVs), are very promising due to their higher efficiency and lower or even zero emissions [1]-[5]. Moreover, regenerative braking systems (RBS) can recover the vehicle's kinetic energy during deceleration, further reducing fuel consumption [6]-[9].

A Cyber-Physical System is a distributed, networked system that fuses computational processes (cyber world) with the physical world. An electrical vehicle is a typical example of CPS [10]. In details, an electric powertrain involves the following subsystems: the controller, representing the "Cyber" world, the physical plant, the driver, the "Human", and the environment. These different parts, which are highly coupled, decide the vehicle and powertrain's behavior and performance [11].

Recent study shows that human driver behaviors, including driving modes, driving styles, and driver-vehicle interactions, exert crucial impacts on the performances of electrified powertrains. In [12], the effect of driving styles on a conventional vehicle platform and the electrical one was compared. The results showed important influence of driving styles in all vehicle platforms. For instance, high-acceleration events have a particularly negative effect on HEVs. Besides, the regenerative braking performance of an electrified powertrain is strongly related to the driver torque request, actuated by the accelerator and brake pedals [13]. The energy efficiency of BEVs can be improved over 20% through regenerative braking. Therefore, small changes in driving mode can cause unnecessary energy waste and sub-optimal vehicle performance [14]. And information of driving scenarios, driver modes, and driver-vehicle interactions is crucial and should be integrated to enhance electric powertrain performance.

The main drawback of the conventional implementations in powertrain design and control is the lack of global optimality in the selection of architecture, parameters, and variables [15]. By using the conventional design flow, which deals with different subsystems independently, even if the controller is very well designed, the improvement of vehicle performance could be limited, since the physical architecture and parameters are not optimized in sync with the controller, and the system potential is not fully explored. Optimal co-design of the physical architecture and controller parameters with human operation consideration provides the ability to extend system design space and improve the overall CPS performances [16]-[19]. However, in addition to the cyber and the physical worlds, we need to include the "Human" side of a vehicle. To do so, the interactions between the physical plant, controller parameters, vehicle performance, and driving mode have to be well understood.

In this paper, we propose a CPS based framework for the optimal co-design of the physical plant parameters and controller variables for an electric powertrain with different driving mode considerations, while taking into account the trade-off between vehicle dynamic performance, ride comfort, and energy efficiency.

The paper is organized as follows: The co-design optimization problem is illustrated in Section II. A cyber-physical optimization framework is proposed and presented in Section III. System models and driving-mode-oriented controller synthesis are described in Section IV. Then, the performance exploration methodology is

Published by SAE.
First online 28 March 2017 at http://papers.sae.org/2017-01-0426/.

proposed in Section V. Section VI reports simulation-based design optimization results, followed by conclusions in Section VII.

Problem Description

In this study, the goal is to formulate the CPS-based intelligent powertrain control under different driving modes for an electric vehicle as a multi-objective optimization problem. Optimal assignments for design variables to maximize performances while satisfying a number of constraints are expected to be found. To ensure that the problem is of a reasonable complexity, only longitudinal vehicle control in normal driving situations is considered, and the sizing of the powertrain system is fixed, i.e., the parameters of the energy source (battery) and the power source (electric motor) are constant to bound the exploration space.

Intelligent Electric Powertrain System

Electric Powertrain System

Figure 1 shows the overall structure of the electrified powertrain system considered in this study. For the physical structure, a central electric motor is installed at the front axle of the vehicle. During acceleration, the electric motor, powered by the battery, provides propulsion through the transmission system to the wheels. During deceleration, the regenerative braking torque generated by the motor is synchronized with the friction brake torque modulated by the hydraulic modulator, in a cooperative regenerative braking function.

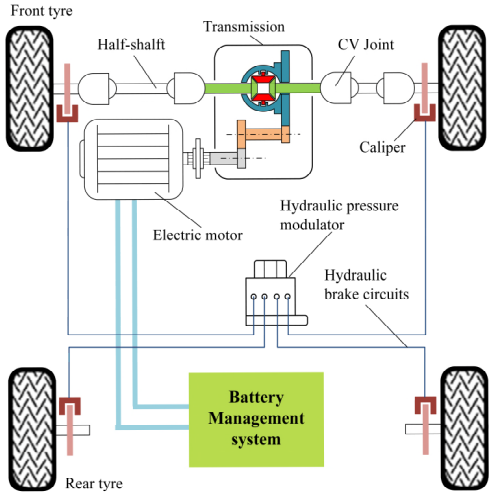

Figure 1. Structure of the electric powertrain physical plant.

Intelligent Powertrain Control Architecture

The high-level powertrain control strategy is designed to output a suitable torque to propel the vehicle, satisfying the longitudinal motion requirement of the vehicle. The output torque demand is generally determined by driver's operation maneuver. Specifically, as Figure 2 shows, in this study, the intelligent powertrain controller is synthesized considering different driving modes, i.e. the requested output torque of the powertrain is not only decided by the driver's operation, but also differentiated by the driving modes. In the implementation phase, the driving mode can be either selected through a human-machine interface (HMI), or identified by smart sensing of driver's intentions or preferences using machine learning approaches. In this work, we assume that the driving mode selection is available via HMI.

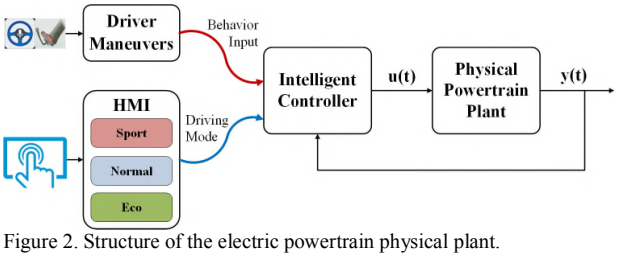

Figure 2. Structure of the electric powertrain physical plant.

Driving Mode

Oriented by the driving-mode-aware intelligent powertrain control described above, three driving modes are considered in this work and defined as follows.

1) Sport: The Sport driving mode exhibits sharp and abrupt accelerations and deceleration, aiming at vehicle dynamic performance. This mode results in higher fuel consumption and increased likelihood of accidents as well.

2) Eco: The driving mode of Eco exhibits a high efficient energy conversion of the powertrain with small amplitudes and low frequency actions on both longitudinal and lateral dynamics. This Eco mode values primarily energy efficiency, avoiding abrupt variation of powertrain torque demand.

3) Normal: The Normal driving mode is in between. It does not aim at absolute vehicle performance, but would like to balance multiple performances, such as vehicle dynamic performance, energy consumption, and ride comfort.

Driving Scenario

In this paper, as mentioned above, we focus on vehicle longitudinal motion control, whereas the lateral motion and dynamics related to the steering wheel operation are not involved. Hence, the following driving scenarios are of importance in our derivations.

1) Scenario 1: 0-50km/h acceleration. In this scenario, the car is accelerated from 0 to 50 km/h. With the intelligent powertrain controller, the motor torque will be generated based on different control strategies and parameter selections corresponding to different driving modes. The vehicle acceleration, jerk, and the time taken in this process are used to evaluate the dynamic performance and ride comfort under different driving modes.

2) Scenario 2: 50-0 km/h deceleration. In this scenario, the car is decelerated from 50 km/h to 0. For an electric car, the total brake demand is distributed to the regenerative and frictional brakes. Different deceleration demands will be generated by the intelligent powertrain controller under different driving modes. The deceleration and the time taken in this process are typical performance indices. The overall energy recovered during the braking process can be used to evaluate energy consumption. This scenario will be used to verify vehicle's performance and energy efficiency during optimization.

3) Scenario 3: standard driving cycle. The standard ECE driving cycle is adopted for measuring energy efficiency since this driving cycle is close to the behavior of a vehicle in an urban area and covers an extended operation time period. This scenario will be used to check vehicle's energy efficiency during optimization.

Vehicle Performance

The performances for vehicle design and control involve safety, dynamical performance, energy efficiency, and ride comfort. Driving mode consideration implies the introduction of trade-offs between multiple performances that are the objective functions in our optimization problem under different driving modes.

1) Dynamic performance: Dynamic performance is the fundamental and the most important indicator of a car. Maximum speed and acceleration time are proxies for dynamic performance. Dynamic performance depends on driver behavior as well as on the parameters of the physical plant and the controller. In this paper, we select the acceleration time and the deceleration time as two indicators for the dynamic performance.

2) Energy efficiency: The energy efficiency of a vehicle can be represented by the fuel or energy consumed during a certain trip. Powertrain performance as well as driving mode have great effects on energy consumption. For electrified vehicles, energy consumption can be significantly enhanced through regenerative braking. Thus, in this paper, we set the regenerated braking energy as one of the optimization goals in the trade-off problem.

3) Ride comfort: During accelerations and decelerations, torsional oscillations may occur in the powertrain due to fast torque transitions, resulting in unexpected jerks at the vehicle level and deteriorated drivability. To cope with this problem, an active damping controller is usually required [20]. Thus, we would like to co-optimize related plant parameters and controller variables to improve comfort level under different driving modes.

Basic Requirements and Limitations

During vehicle design, control, and optimization, there are some basic requirements and limitations of the physical systems that need to be taken into account.

1) Maximum vehicle speed: The maximum speed of the vehicle is determined by the highest rotational speed of the electric motor, the radius of tire, and the gear ratio.

2) Minimum gradeability: Gradeability is defined as the highest grade a vehicle can ascend maintaining a particular speed. It is an important requirement in vehicle design.

3) Minimum brake intensity: In order to guarantee stability during braking, a vehicle needs to have enough braking force, represented by the brake intensity z, as required by regulation ECE-R13 [21].

4) Powertrain limitation: Once the sizing of the power source is given, then the output torque of the powertrain is bounded by the outer characteristics profile of the electric drive.

Cyber-Physical Optimization Framework

The optimization problem is a constrained multi-objective optimization problem where both vehicle and controller parameters need to be optimally chosen. In this paper, we adopt as co-design methodology Platform-Based Design (PBD) [10]. As Figure 3 shows, PBD is a meet-in-the-middle approach that favors re-usability. At the top layer are high-level requirements and constraints, which are characterized by driving modes, driver maneuvers, and driving scenarios. The bottom layer is defined by a design platform, i.e., a library of components characterized by their behaviors and performance. The bottom layer contains the models of the electric powertrain, the brakes, and the driver-mode-aware controller. The models are parameterized to capture families of vehicles, powertrains, brakes and controllers. The design problem is to select a set of components and their parameters so that the constraints are satisfied and the objective functions optimized. The selection process is called mapping, indicated as the meeting point in the diagram, since the obligations captured in the requirements and constraints are discharged by particular components or combinations thereof. Co-design of the physical plant parameters, controller protocols and variables, for the intelligent electric powertrain is then made possible.

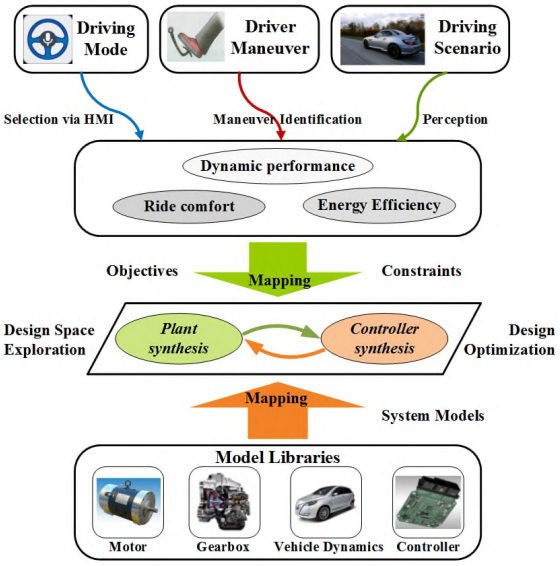

Figure 3. PBD-based optimization framework for electrified powertrain.

System Modelling and Formulation

The following model and formulation is able to support interactive performance exploration and optimization between components at different layers within a unifying framework.

System Modelling

Electric Powertrain Model

Oriented by controller synthesis and optimization, the powertrain is simplified to a two-inertia model, as presented in Figure 4. One inertia corresponds to the electric motor, and the other corresponds to the contribution by the wheels. The gearbox, consisting of the

transmission, final drive, differential, and inner and outer constant-velocity (CV) joints, is located close to the motor inertia.

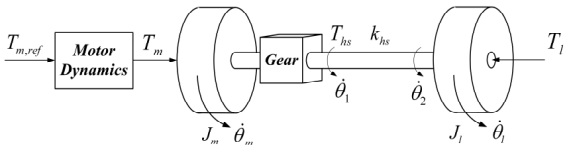

Figure 4. Structure of the simplified powertrain system model.

Assuming that the half shafts are of the same length, the motor output torque is considered to be equally distributed over the left and right half shafts. The motor torque is modelled as a first-order reaction, as shown in equation (1). The transmitted torque via the gearbox can be represented by equation (2). The model for the half-shaft torque can be given by equation (3).

$$T_{m,ref} = T_m + \tau_m \dot{T}_m \tag{1}$$

$$J_m \ddot{\theta}_m = T_m - 2T_{hs}/i_g \tag{2}$$

$$T_{hs} = k_{hs}(\theta_m / i_g - \theta_w) + c_{hs}(\dot{\theta}_m / i_g - \dot{\theta}_w) \tag{3}$$

where, τ_m is the small time constant, T_{hs} is the half-shaft torque, J_m is the motor inertia, and θ_m and θ_w are the angular positions of electric motor and load, respectively. Furthermore, k_{hs} and c_{hs} are the stiffness coefficient and damping coefficient of the half shaft, respectively.

The energy source, i.e. the battery, is built as an open-circuit voltage-resistance model based on the data of the lithium-ion battery utilized in a commercial electric vehicle. In this paper, look-up tables are compiled on the basis of the state of charge (SOC) and temperature data for the battery, modeling its charging-discharging internal resistance. The model's input is the power required by the electric motor, and its outputs include the SOC, the voltage at the output port, the current, and the temperature of the battery. The detailed model with parameters can be found in [6].

Regenerative Brake Model

In this paper, the brake force distribution (BFD) ratio β is set to a fixed value, which can be obtained by the parameters of the brake devices. The front and rear brake demand can be calculated as follows.

$$T_b = 2T_{b,fw} + 2T_{b,rw} \tag{4}$$

$$T_{b,fw} = \frac{\beta}{2} \cdot T_{b,dmd} \tag{5}$$

$$T_{b,rw} = \frac{1-\beta}{2} \cdot T_{b,dmd} \tag{6}$$

where T_b is the actual braking torque provided by the blended brakes, $T_{b,dmd}$ is the demanded braking torque of the vehicle, and $T_{b,fw}$ and $T_{b,rw}$ are the brake torque of one front wheel and one rear wheel, respectively.

Vehicle Longitudinal Model

Because we focus on the longitudinal motion of the vehicle, the vehicle model adopts the longitudinal dynamics model:

$$m\dot{v} = \frac{2T_{hs}}{r} - \frac{T_b}{r} - fmg - \frac{1}{2}C_D A \rho v^2 \tag{7}$$

where m is the vehicle mass, v is the vehicle speed, r is the nominal radius of tire, C_D is the coefficient of air resistance, A is the frontal area, and ρ is the air density.

Some key parameters of the case study electric vehicle are listed in Table 1.

Table 1. Key parameters of the electric powertrain and vehicle.

	Parameter	Value	Unit
Electric powertrain	Peak power	40	kW
	Maximum torque	145	Nm
	Maximum speed	9000	rpm
	Gear ratio	7.881	—
Vehicle	Total mass (m)	1360	kg
	Wheel base (L)	2.50	m
	Coefficient of air resistance (C_D)	0.32	—
	Nominal radius of tyre (r)	0.295	m

Driving-Mode-Aware Intelligent Controller Design

As Figure 5 represented, the high-level supervisory controller adopts a scheduling protocol, requesting the control architecture and objectives of the low-level controller, as well as parameters to the physical plant, dynamically adapts to different driving modes.

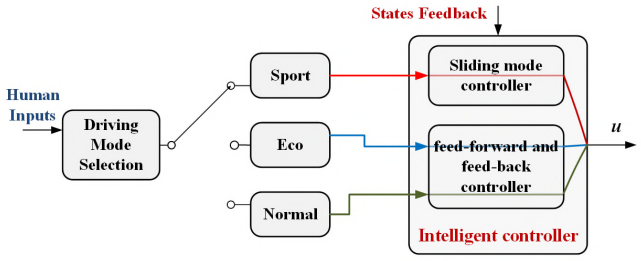

Figure 5. Scheduling protocol of the driving-mode-aware controller.

Sport-Mode Powertrain Control

Based on the sporty feature of this driving mode, the vehicle longitudinal control under this condition can be seen as an acceleration tracking problem, realizing the sporty feel of the driving for passengers. The control objective is to track the reference acceleration using the actual one. Because of its ability to address nonlinearity and fast response [22], a sliding-mode control (SMC) scheme is applied, as shown in Figure 6(a).

In designing the sliding-mode controller, an integral-type sliding surface S is chosen with the error term *e* defined in equations (8) and (9).

$$S = \int e dt \tag{8}$$

$$e = a - a_{ref} \tag{9}$$

where a and a_{ref} are the actual and reference values of the vehicle acceleration, respectively.

Lyapunov direct method is used to design a control law that derives the system trajectories to the sliding surface [23]. The following function is used for the system:

$$V = \frac{1}{2} SS \tag{10}$$

To ensure the stability of the system, the derivative of the Lyapunov function should satisfy the following condition [24]:

$$\dot{V} = S\dot{S} \le 0 \tag{11}$$

Then, combining the above equations, when $\dot{S} = 0$, the SMC control law can be derived. Besides, to avoid the chattering caused by the discontinuous sign function, sgn(*S*), in the standard SMC, a continuous function S is utilized instead of the discontinuous term, as shown in equation (12) [25].

$$T_{m,ref} = mr\left(a_{ref} + fg + \frac{C_D A \rho v^2}{2m} - k_{SMC} S \right) \tag{12}$$

where k_{SMC} is the positive gain of the SMC controller.

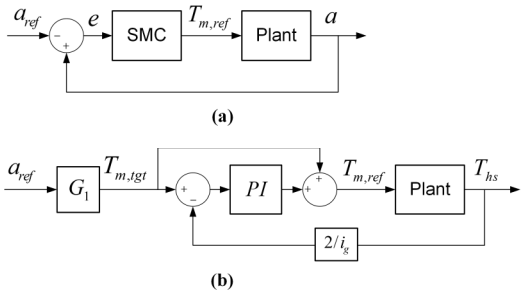

Figure 6. Diagram of the powertrain controller for different driving modes.

Eco-Mode Powertrain Control

In this mode, the acceleration and deceleration operations of the vehicle become significantly milder. It features high energy efficiency with smooth driving maneuvers. To this end, the powertrain controller uses a combined feed-forward and feed-back structure, as shown in Figure 6(b), in order to actively damp powertrain torsional vibrations, reducing the power consumption during torque transient process. Based on the control objective, the feed-forward term can be determined by the target motor torque $T_{m,tgt}$,, which can be calculated using the reference acceleration. For the feedback term, a linear proportional-integral (PI) controller is adopted to damp the torsional oscillation.

$$T_{m,ref} = T_{m,tgt} + (K_P + K_I \int dt) \cdot e \tag{13}$$

$$e = T_{m,tgt} - 2T_{hs} / i_0 i_g \tag{14}$$

where the feedback gains K_P and K_I are tuning parameters of the PI controller.

Normal-Mode Powertrain Control

In the normal driving mode, the operators usually care more about energy efficiency and smooth driving. In this condition, the low-level powertrain controller adopts the same combined feed-forward and feed-back architecture as for the Eco-mode to ensure vehicle drivability and energy efficiency.

Performance Representation

1) Dynamic performance: In this paper, we select the 0-50 km/h acceleration time t_{acc} and the 50-0 km/h deceleration time t_{brk} as two indicators for the dynamic performance to capture driver's behavior including the selection of suitable values for the gear ratio i_g.

2) Energy efficiency Representation: In this paper, we set the regenerated braking energy defined in equation (15) as one of the optimization goals in the trade-off problem [26].

$$E_{reg} = \eta_{gen} \cdot \int T_{m,reg} \omega_m dt \tag{15}$$

where E_{reg} is the regenerated braking energy, $T_{m,reg}$ and ω_m are the regenerative brake torque and the angular speed of the electric motor, respectively, and the η_{gen} is the generation efficiency of the motor.

3) Ride comfort representation: The comfort level of a vehicle can be assessed considering vehicle's jerk *j*, which is the second derivative of the vehicle longitudinal velocity *v* [6]. Typically, for reaching a good comfort level, the vehicle's maximum longitudinal jerk should be no more than 15 m/s^3.

$$j = \ddot{v} \tag{16}$$

Constraint Formulation

1) Maximum vehicle speed. The constraint on vehicle speed is posed as:

$$v_{\max} = \frac{r\pi n_{\max}}{30 i_g} \ge (100/3.6)\, m/s \tag{17}$$

where $v_{\max}$ is the maximum speed of the vehicle, $n_{\max}$ is the highest rotational speed of the electric motor, and the i_g is the gear ratio.

2) Gradeability. Given the electric motor capability, the gradeability performance can be determined by the gear ratio, which is represented as:

$$\eta_t i_g T_{m,\max} = mgr(f\cos\alpha_{\max} + \sin\alpha_{\max}) \quad (18)$$

$$i_{\max} = \tan\alpha_{\max} \geq 30\% \quad (19)$$

where η_t is the trainsmission efficiency, $T_{m,max}$ is the maximum torque of the electric motor, f is the friction drag coefficient, r is the nominal radius of tire, and the α is the grade angle.

3) Minimum brake intensity: The brake intensity required by regulation ECE-R13 can be given by [21]:

$$z = \frac{\dot{v}}{g} \geq 0.1 + 0.85(\varphi - 0.2) \quad (20)$$

where φ is the adhesion coefficient of the road.

4) Powertrain limits: The limitation set by the electric powertrain can be represented as follows:

$$T_m \omega_m \leq P_{m,lim} \quad (21)$$

where $P_{m,lim}$ is the output power limit of the electric motor.

Driving-Mode Aware Performance Optimization

Design Space Exploration

Based on the assumptions and constrains formulated in Section II, namely requirements for vehicle safety, vehicle speed, gradeability, and powertrain capability, the boundaries of related physical plant parameters, i.e., upper and lower limits of the gear ratio i_g and BFD ratio β, are determined as follows. The design space is then bounded to this region.

$$7.708 \leq i_g \leq 9.330 \quad (22)$$

$$0.60 \leq \beta \leq 0.80 \quad (23)$$

Simulation Based Performance Exploration

In order to carry out multi-objective optimization under different driving modes, the impacts of the related parameters on the performance indicators and their interactions should be explored. In this paper, we propose a simulation-based exploration algorithm to do so. Assuming that, within the Parameter Library ξ, there are four parameters, including parameters of the physical plant and controller variables, deciding one performance. Under pre-defined driving scenario within valid design space, the selected vehicle performance is simulated in the Simulink environment stepping each parameter with a suitably small step. After global simulation-based exploration, the best performance with its corresponding value selections of the parameters can be attained. The overall flow of the optimization procedure under each driving mode is shown in Figure 7. And the detailed algorithm can be found in the Appendix.

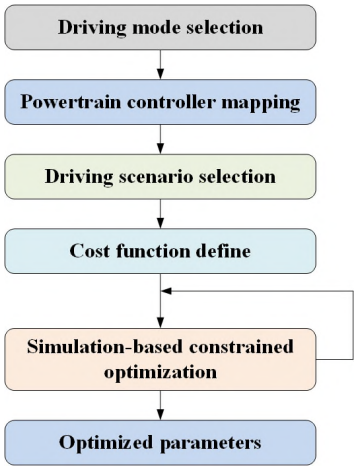

Figure 7. Overall flow of the CPS-based optimization procedure.

Driving-Mode-Aware Multi-Objective Optimization

1) Sport-mode optimization: This driving mode requires to maximize vehicle dynamical performance first and foremost. In addition, we wish also to guarantee a good performance in terms of energy efficiency. Therefore, we consider the trade-off between dynamic performance and energy efficiency, with a much greater weight on the side of dynamic performance. The cost function is designed as:

$$J = \min_{-E_{reg}} \left(\omega_1 \cdot t_{acc} + \omega_2 \cdot t_{brk} - \omega_3 \cdot E_{reg} \right) \quad (24)$$

Thus, within the cost function, the parameters of the powertrain system to be optimized are: i_g, k_{SMC}, β.

2) Eco-mode optimization: As mentioned above, under the eco driving mode, the drivers are usually with the intentions of saving energy and ensuring comfortable driving. Thus, for the multiple objective system optimization, the trade-off elements are now energy and efficiency ride comfort. The parameters to be optimized are: i_g, K_P, K_I, β.

$$J = \max_{E_{reg}} \left(\omega_1 \cdot E_{reg} - \omega_2 \cdot j \right) \quad (25)$$

3) Normal-mode optimization: In this case, the multi-objective optimization problem is a trade-off between dynamic performance and ride comfort. The cost function for this mode is designed as follows. And the parameters to be optimized are: i_g, K_P, K_I, β

$$J = \min_{j} \left(\omega_1 \cdot j + \omega_2 \cdot t_{acc} - \omega_3 \cdot E_{reg} \right) \quad (26)$$

The detailed weighting set-up for the objective functions of the three driving modes is summarized in Table 2.

Table 2. Weighting set-up for the objective functions under different modes.

Driving Mode	Weights

	ω_1	ω_2	ω_3
Sport	5	5	2
Eco	1	1	0
Normal	5	5	1

Optimization Results and Analyses

The above system models, optimization goals, requirements, and formulated constrains are embedded in the Matlab/Simulink environment, driving the implementation of the multi-objective performance optimization for the intelligent powertrain system.

Optimization Results for Sport-Mode

Based on the cost function designed for the sport mode, we explore the interactive effects of the values of the SMC gain, the gear ratio, and BFD on the dynamic performance of the 0-50km/h acceleration and regenerated braking energy. According to the exploration results shown in Figure 8, the positive gain of the SMC controller k_{SMC} tends to be small, while the gear ratio prefers a larger value in favor of a better acceleration performance. For the regenerative braking performance, β needs to select a small value to reach a higher efficiency according to the exploration results.

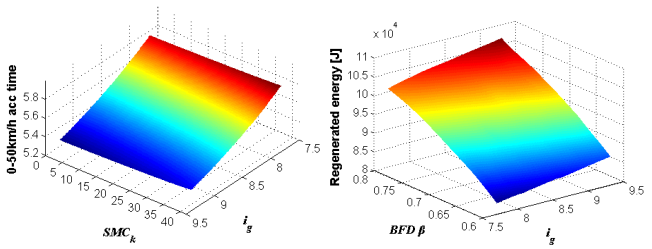

Figure 8. Performance exploration results of the sport driving mode.

Optimization Results for Normal-Mode

Based on the multiple optimization objectives of the normal driving mode, the trade-off between ride comfort and vehicle acceleration performance is considered. As an example, the exploration results under the gear ratio of 8.3 are shown in Figure 9. The gains selection of the PI controller has a great impact on vehicle jerk. While the manipulation of the gains of the PI active damping controller has very small influence on the energy regeneration performance, according to the exploration results. The detailed optimization results for parameter selection are summarized in Table 3.

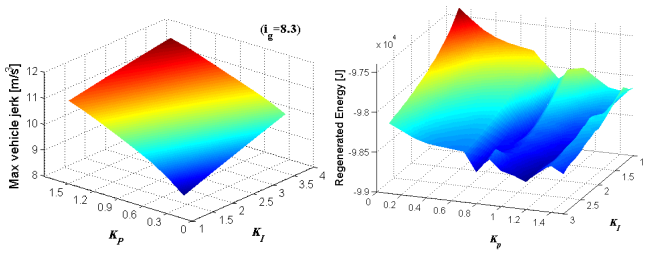

Figure 9. Performance exploration results of the normal driving mode.

Optimization Results for Eco-Mode

Since the controller structure of the eco mode is the same with the normal one, the related parameters which to be optimized are the same. However, because the optimization objectives are different under these two modes, the value selections of those parameters at the end of the optimization process can be far different, as shown in Figure 10. The generated optimization results of the parameters selection are listed in Table 3.

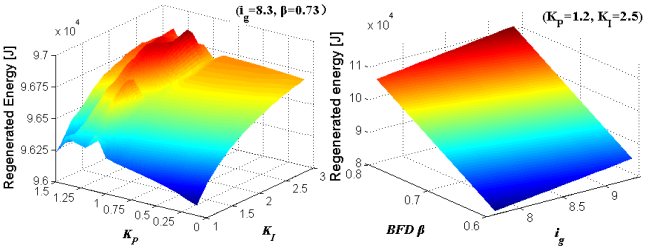

Figure 10. Performance exploration results of the eco driving mode.

Table 3. Optimized parameter for different driving modes.

Driving mode	Optimized parameters				
	i_g	β	k_{SMC}	K_P	K_I
Sport	9.012	0.641	2.5	-	-
Eco	8.281	0.79	-	0.01	0.12
Normal	8.563	0.725	-	1.30	2.35

Comparison of Results under Different Modes

Comparisons of the results under different modes is shown in Figure 11. The sport mode, which favors dynamic performance, dominates the acceleration and deceleration events among the three. The eco mode, which is in favor of energy efficiency, as well as the ride comfort, reaches the best performance in regenerative braking and jerk reduction. Finally, the normal mode, which sits in between the above two, achieves a good balance between dynamic performance, ride comfort, and energy efficiency.

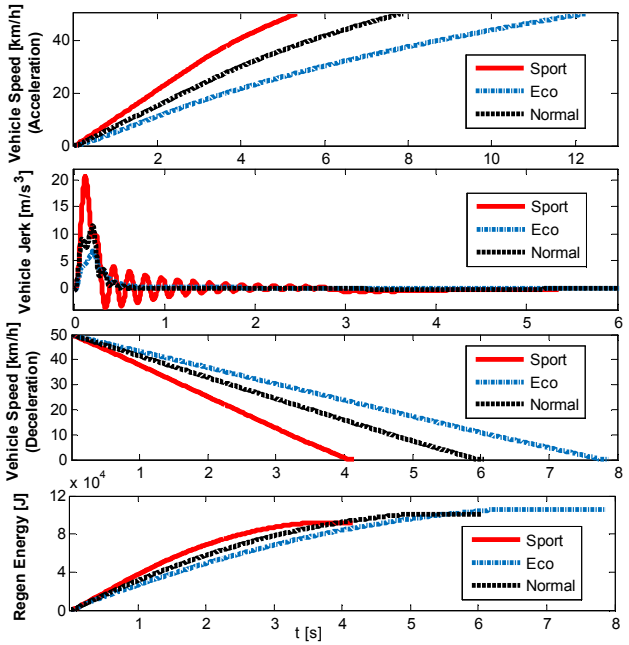

Figure 11. Comparison of results under different driving modes.

To compare the energy efficiency at the vehicle level with different modes, simulations under the standard ECE driving cycle are performed. The reference speed profile is shown in Figure 12. According to the results listed in Table 4, the energy consumption of the vehicle under the Eco mode is 575.9 kJ, which improves the energy efficiency by over 10%, compared to the energy utilization of sport mode.

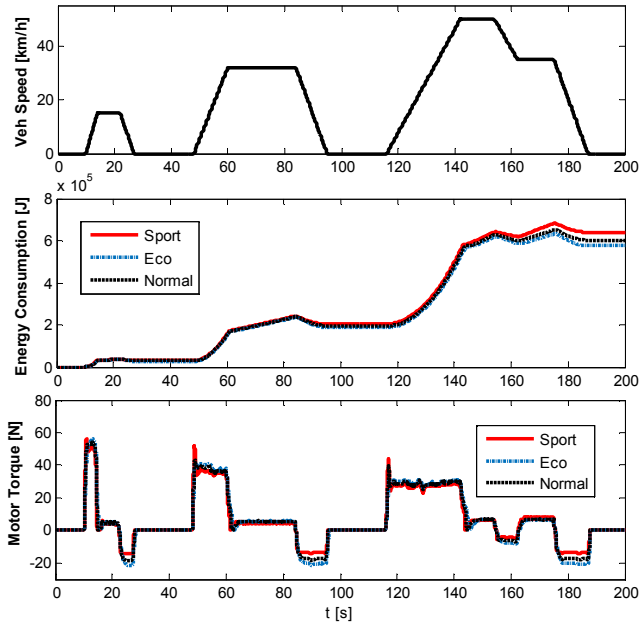

Figure 12. Simulations results under the standard ECE driving cycle.

Table 4. Simulation results of energy efficiency under ECE driving cycle.

Driving mode	Regenerated energy [kJ]	Consumed energy [kJ]
Sport	91.7	640.6
Eco	106.0	575.9
Normal	100.4	601.9

Conclusions

In this paper, we proposed a cyber-physical system-based framework for the optimal co-design of the intelligent electrified powertrain system under three driving modes, namely the sport, the eco, and the normal modes. The system architecture, objective performances and system constraints, optimization goals and methodology were presented. A performance exploration methodology and algorithm were proposed. Scheduling based intelligent powertrain control algorithms were synthesized for the three driving modes. Simulation results show that electric powertrain with optimized parameters using the proposed methodology can perform well in three different driving modes. Moreover, the overall performance considering vehicle dynamics, ride comfort, and energy efficiency is significantly improved with the co-design of the parameters. Simulation results demonstrate the advantages of the proposed framework over a conventional benchmark.

Future work will include vehicle test of the proposed optimization method, and consideration of different driving styles and driver intentions.

References

1. Chau, K.T., Chan, C.C. Emerging energy-efficient technologies for hybrid electric vehicles. Proceedings of the IEEE, 2007, 95(4): 821-835.
2. Crolla, D. A., Cao, D. The impact of hybrid and electric powertrains on vehicle dynamics, control systems and energy regeneration. Vehicle system dynamics, 50(sup1): 95-109, 2012.
3. Hu, X., Jiang, J., Cao, D., Egardt, B. Battery health prognosis for electric vehicles using sample entropy and sparse Bayesian predictive modeling. IEEE Transactions on Industrial Electronics, 63(4): 2645-2656, 2016.
4. Martinez, C.M., Hu, X., Cao, D., et al. Energy Management in Plug-in Hybrid Electric Vehicles: Recent Progress and a Connected Vehicles Perspective, IEEE Transactions on Vehicular Technology, in press, 2016.
5. Hu, X., Jiang, J., Egardt, B., Cao, D. Advanced power-source integration in hybrid electric vehicles: Multicriteria optimization approach. IEEE Transactions on Industrial Electronics, 62(12): 7847-7858, 2015.
6. Zhang, J., Lv, C., Gou, J., Kong, D. Cooperative control of regenerative braking and hydraulic braking of an electrified passenger car. Proceedings of the Institution of Mechanical Engineers Part D Journal of Automobile Engineering, 2012, 226(10): 1289-1302.
7. Lv, C., Zhang, J., Li, Y. Extended-Kalman-filter-based regenerative and friction blended braking control for electric vehicle equipped with axle motor considering damping and

elastic properties of electric powertrain. Vehicle System Dynamics, 2014, 52(11): 1372-1388.
8. Lv, C., Zhang, J., Li, Y., Yuan, Y. Mode-switching-based active control of powertrain system with nonlinear backlash and flexibility for electric vehicle during regenerative deceleration. Proceedings of the Institution of Mechanical Engineers Part D Journal of Automobile Engineering, 2015, 229(11): 1429-1442.
9. Lv, C., Zhang, J., Li Y., et al. Hardware-in-the-loop simulation of pressure-difference-limiting modulation of the hydraulic brake for regenerative braking control of electric vehicles, Proceedings of the Institution of Mechanical Engineers. Part D: Journal of Automobile Engineering, 228(6):649-662, 2014.
10. Nuzzo, P., Sangiovanni-Vincentelli, A. L., Bresolin, D., Geretti, L., Villa, T. A platform-based design methodology with contracts and related tools for the design of cyber-physical systems. Proceedings of the IEEE, 103(11): 2104-2132, 2015.
11. Lv, C., Zhang, J., Nuzzo, P., Sangiovanni-Vincentelli, A., Li, Y., Yuan, Y. Design optimization of the control system for the powertrain of an electric vehicle: A cyber-physical system approach. IEEE International Conference on Mechatronics and Automation (ICMA), 2015.
12. Neubauer, J. Wood, E., "Accounting for the Variation of Driver Aggression in the Simulation of Conventional and Advanced Vehicles," SAE Technical Paper 2013-01-1453, 2013, doi:10.4271/2013-01-1453.
13. Lv, C., Zhang, J., Li, Y., Yuan, Y. Directional-stability-aware brake blending control synthesis for over-actuated electric vehicles during straight-line deceleration. Mechatronics, 2016.
14. Syed, F., Nallapa, S., Dobryden, A., Grand, C. et al., "Design and Analysis of an Adaptive Real-Time Advisory System for Improving Real World Fuel Economy in a Hybrid Electric Vehicle," SAE Technical Paper 2010-01-0835, 2010, doi:10.4271/2010-01-0835.
15. Kawamura, H., Ito, K., Karikomi, T., and Kume, T., "Highly-Responsive Acceleration Control for the Nissan LEAF Electric Vehicle," SAE Technical Paper 2011-01-0397, 2011, doi:10.4271/2011-01-0397.
16. Sangiovanni-Vincentelli, A., Damm, W., Passerone, R. Taming Dr. Frankenstein: Contract-based design for cyber-physical systems. European journal of control, 18(3): 217-238, 2012.
17. Derler, P., Lee, E. A., Vincentelli, A. S. Modeling cyber-physical systems. Proceedings of the IEEE, 100(1): 13-28, 2012.
18. Sangiovanni-Vincentelli, A. Quo vadis, SLD? reasoning about the trends and challenges of system level design. Proceedings of the IEEE, 95(3), 467-506, 2007.
19. Nuzzo, P., Xu, H., Ozay, N., Finn, J. B., Sangiovanni-Vincentelli, A. L., Murray, R. M., et al. A contract-based methodology for aircraft electric power system design. IEEE Access, 2: 1-25, 2014.
20. Lv, C., Zhang, J., Li, Y., Yuan, Y., "Synthesis of a Hybrid-Observer-Based Active Controller for Compensating Powetrain Backlash Nonlinearity of an Electric Vehicle during Regenerative Braking," SAE Int. J. Alt. Power. 4(1):190-198, 2015, doi:10.4271/2015-01-1225.
21. Gao, Y. and Ehsani, M., "Electronic Braking System of EV And HEV---Integration of Regenerative Braking, Automatic Braking Force Control and ABS," SAE Technical Paper 2001-01-2478, 2001, doi:10.4271/2001-01-2478.
22. Song, B., Hedrick, J. K. Dynamic surface control of uncertain nonlinear systems: an LMI approach. Springer, 2011.
23. Hedrick J.K., Yip P.P., Multiple sliding surface control: Theory and Application, Journal of Dynamic Systems Measurement and Control, 122(4):586-593, 2000.
24. Lv, C., Zhang, J., Li, Y., Yuan, Y. Novel control algorithm of braking energy regeneration system for an electric vehicle during safety–critical driving maneuvers. Energy Conversion and Management, 106: 520-529, 2015.
25. Fazeli A, Zeinali M and Khajepour A. Application of adaptive sliding mode control for regenerative braking torque control. IEEE/ASME Transactions on Mechatronics, 2012, 17: 745-755.
26. Lv, C., Zhang, J., Li, Y., Yuan, Y. Mechanism analysis and evaluation methodology of regenerative braking contribution to energy efficiency improvement of electrified vehicles. Energy Conversion and Management, 92: 469-482, 2015.

Contact Information

Dr. Lv, Chen
State Key Laboratory of Automotive Simulation and Control, Jilin University, Changchun, China;
Advanced Vehicle Engineering Centre, Cranfield University, UK.
Email: c.lyu@cranfield.ac.uk

Dr. Wang, Hong
Department of Mechanical and Mechatronics Engineering, University of Waterloo, Canada.
Email: h492wang@uwaterloo.ca

Mr. Bolin Zhao
Mechanical Engineering Department, Eindhoven University of Technology, The Netherlands.
Email: b.zhao@student.tue.nl

Dr. Cao, Dongpu
Advanced Vehicle Engineering Centre, Cranfield University, UK.
Email: d.cao@cranfield.ac.uk

Dr. Wang, Huaji
Advanced Vehicle Engineering Centre, Cranfield University, UK.
Email: huaji.wang@cranfield.ac.uk

Prof. Zhang, Junzhi
State Key Laboratory of Automotive Safety and Energy, Tsinghua University, Beijing, China;
Collaborative Innovation Center of Electric Vehicles in Beijing.
Email: jzhzhang@mail.tsinghua.edu.cn

Dr. Li, Yutong
State Key Laboratory of Automotive Safety and Energy, Tsinghua University, Beijing, China.
Email: wilson420813@gmail.com

Dr. Yuan, Ye
State Key Laboratory of Automotive Safety and Energy, Tsinghua University, Beijing, China.
Email: yeyuan_91@126.com

Abbreviations

BEV	Battery electric vehicles
BFD	Brake force distribution
CPS	Cyber-physical system
FCEV	Fuel cell electric vehicles
HEV	Hybrid electric vehicle
HMI	Human-machine interface
RBS	Regenerative braking system
PBD	Platform-based design
PHEV	Plug-in hybrid electric vehicles
PI	Proportional-integral
SMC	Sliding mode control
SOC	State of charge

Appendix

As shown in Table 5, assuming that, within the Parameter Library ξ, there are four parameters, namely P_1, P_2, C_1, and C_2, deciding one powertrain performance. Under pre-defined driving Scenario E with valid design space, the selected performance is simulated stepping each parameter with a suitably small step. After global simulation-based exploration, the *Best Performance K* with its corresponding value selections of the parameters can be attained.

Table 5. Algorithm for performance exploration.

Algorithm 1: Performance Exploration

Input: Parameter Library $\{P_1, P_2, C_1, C_2\} \subseteq \xi$, Scenario E
Output: Best Performance Point K

```
1: function Global Exploration (ξ, E)
3: Performance ← {}; Paras ← {};
4: while p1 ∈ P1 do
5:       while p2 ∈ P2 do
6:             while c1 ∈ C1 do
7:                   while c2 ∈ C2 do
8:                         Performance ← Simulation (E, P1, P2, C1, C2)
9:                   end while
10:                        Paras ← Performance (C2);
11:            end while
12:                  Paras ← Performance (C1,C2);
13:      end while
14:            Paras ← Performance (P2,C1,C2);
15: end while
16:     Paras ← Performance(P1, P2, C1, C2);
17:     K ← Best Performance Point (Paras);
        Return K, Paras
18: end function
```

2017-03-28

Cyber-physical system based optimization framework for intelligent powertrain control

Lv, Chen

Society of Automotive Engineers

Lv C, Wang H, Zhao B, et al., (2017) Cyber-physical system based optimization framework for intelligent powertrain control. SAE International Journal of Commercial Vehicles, Volume 10, Issue 1, pp. 254-264, SAE TP 2017-01-0426

http://papers.sae.org/2017-01-0426/